

Discussion of evidences for dextral transpression in the Eastern Cordillera.

There are several independent lines of evidence for the overall dextral transpression controlling the deformation of the Eastern Cordillera-Llanos foreland basin system, including results of plate reconstructions, character of paleostress and present-day stress fields, along-strike migration of the depocenters in the foreland basin and analogy with analog material modeling.

The control of the overall dextral transpression regime in the Northern Andes are roughly northeast- to eastward movements of the Caribbean, Nazca and Cocos plates with respect to the South American plate, which was reconstructed in numerous plate reconstructions addressing this region (e.g., Pindell, 1993; **Fig. 1**; Scotese, 1998; Golonka, 2000; Dalziel *et al.*, 2001). **Fig. 1** shows a series of reconstruction steps made by Pindell (1993) showing the activity of overall dextral transpressional regime in the Northern Andes from the Paleocene till the present. A similar tectonic scenario is shown in an animation authored by Dalziel *et al.* (2001), which is also included.

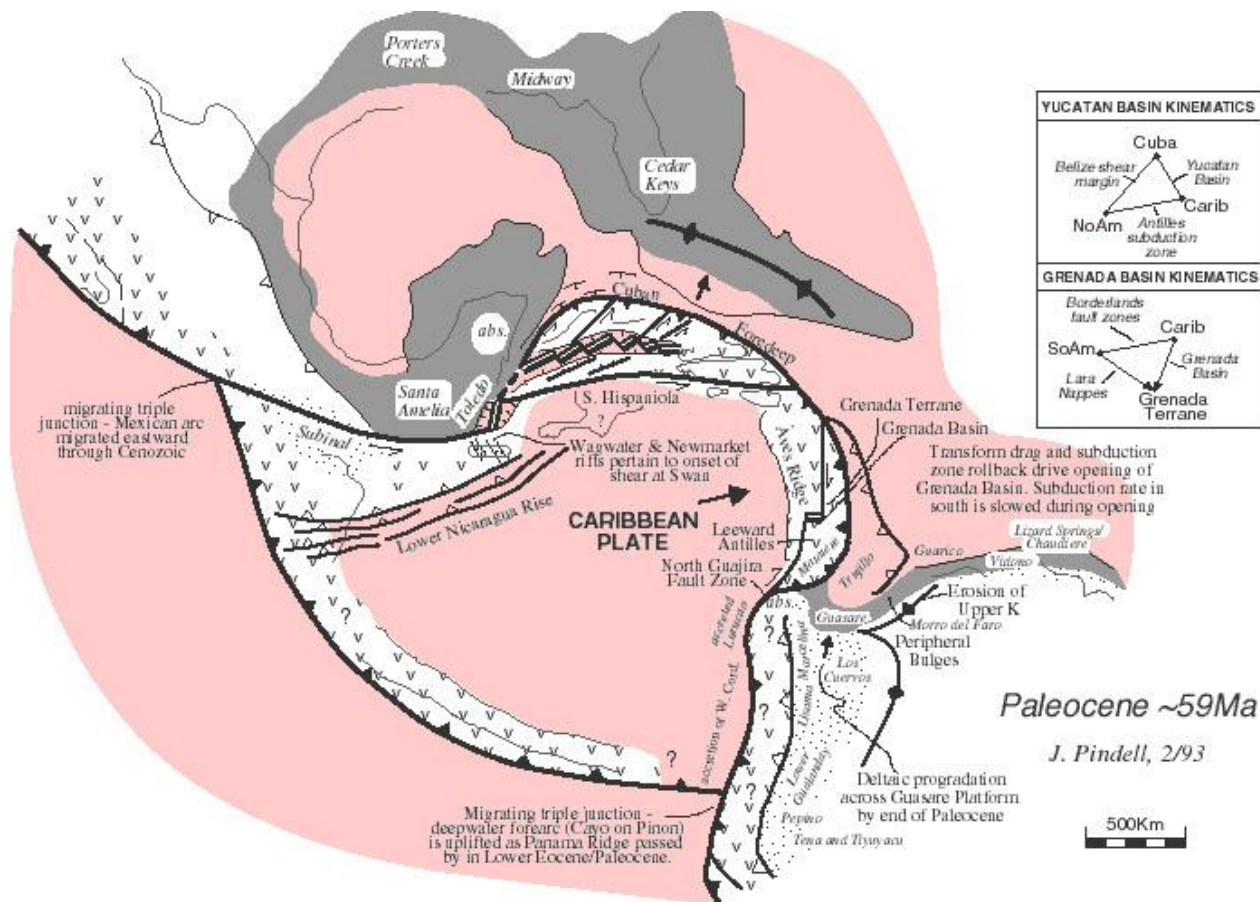
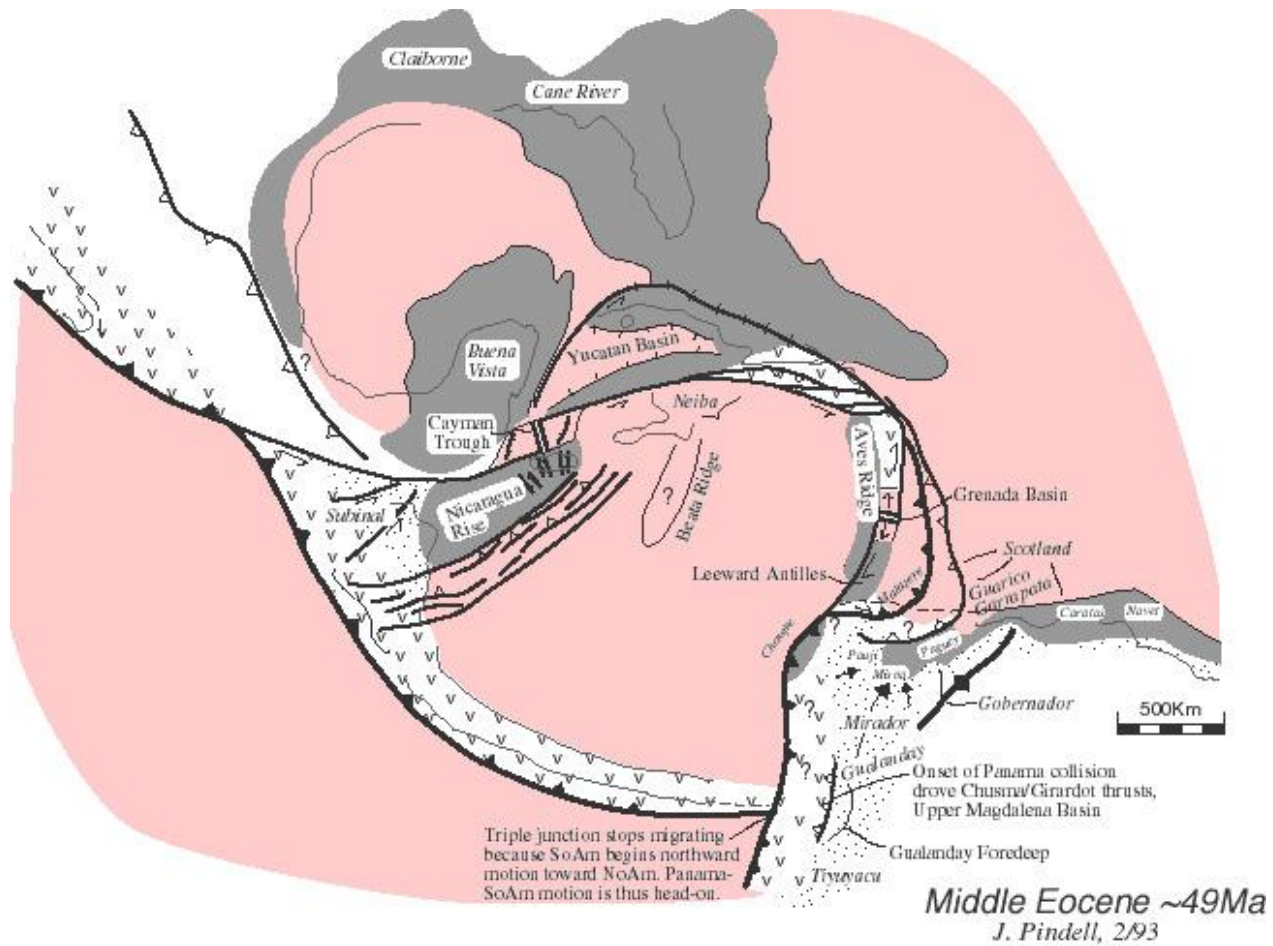
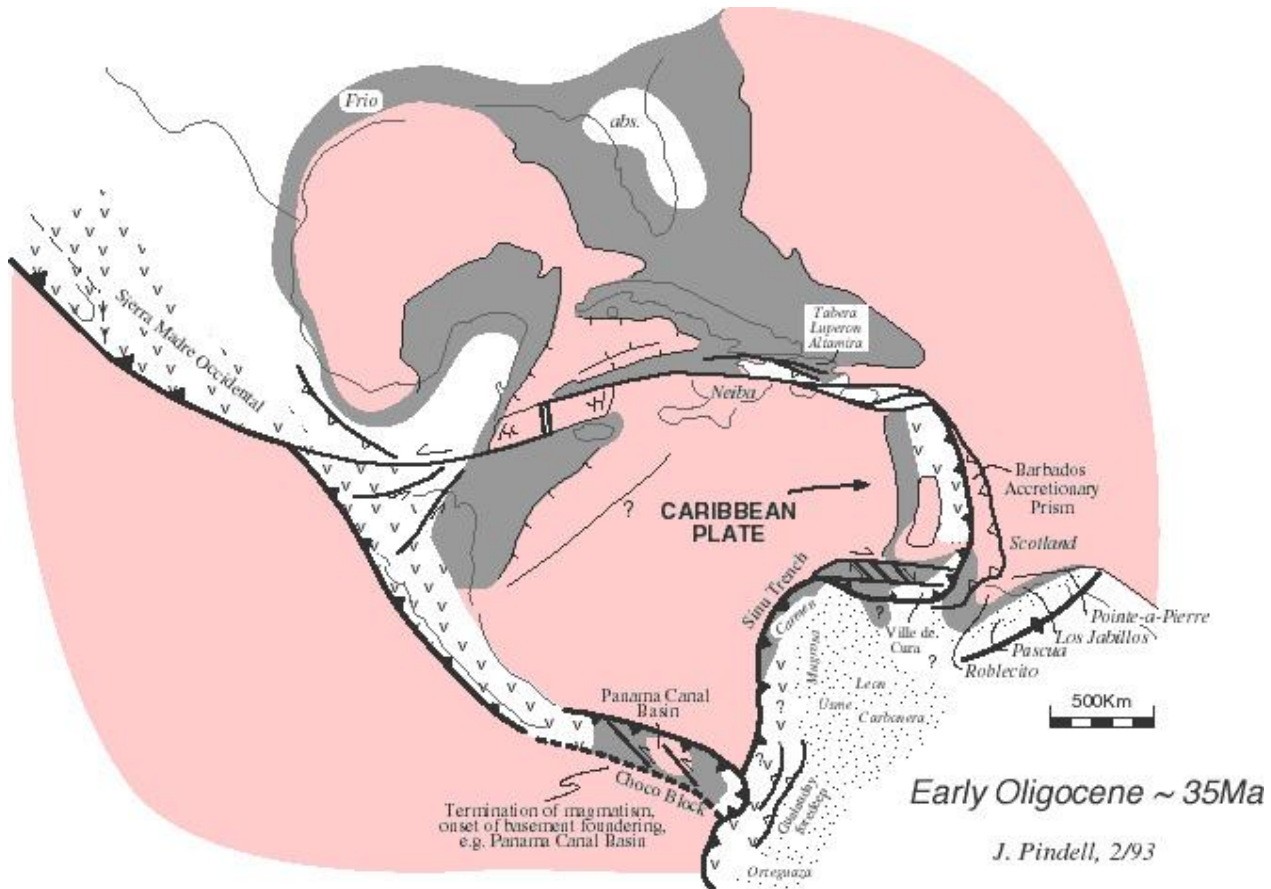


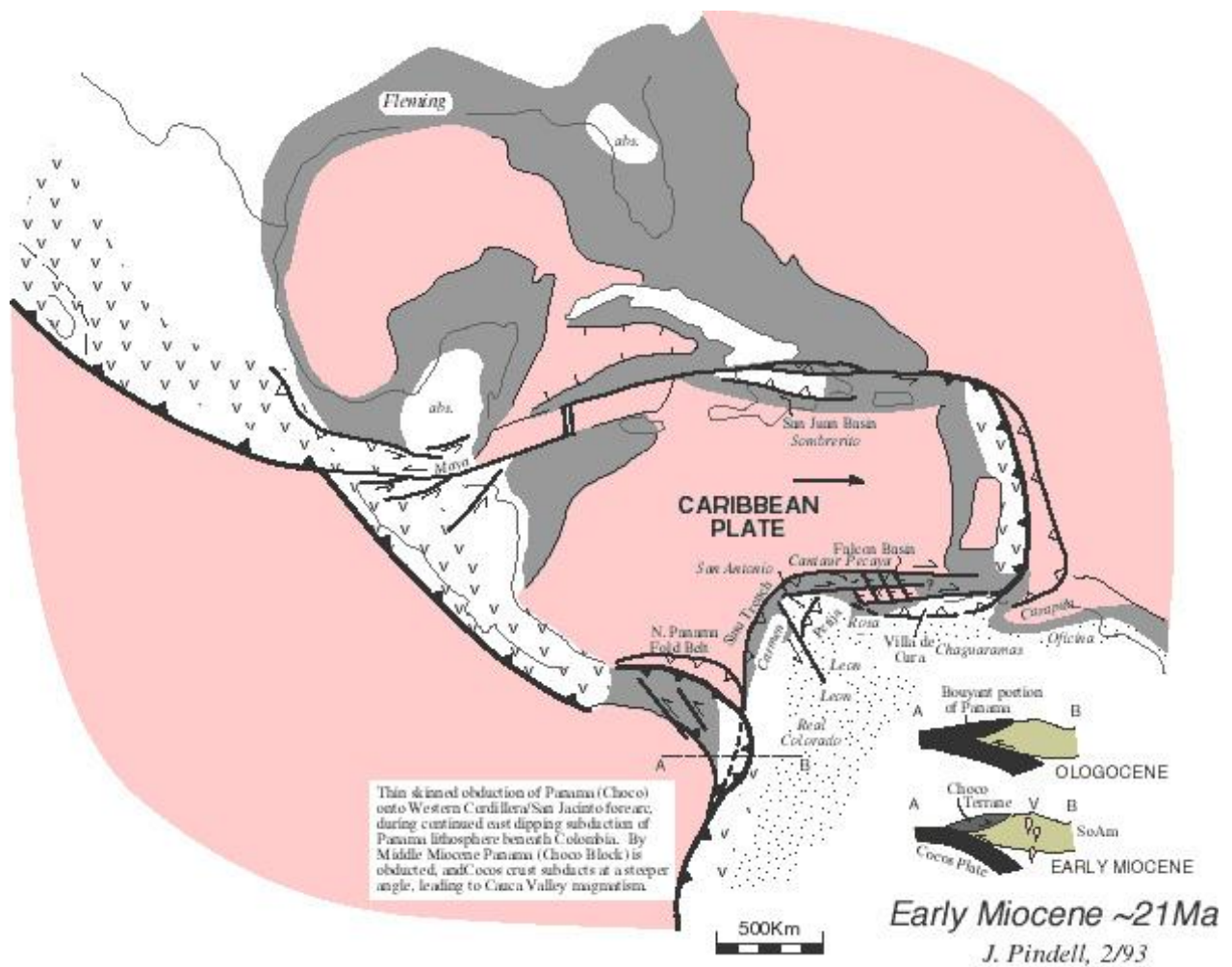
Fig. 1. a) Paleocene stage (59 Ma) of the plate reconstruction done for the circum-North Andean region (Pindell, 1993).



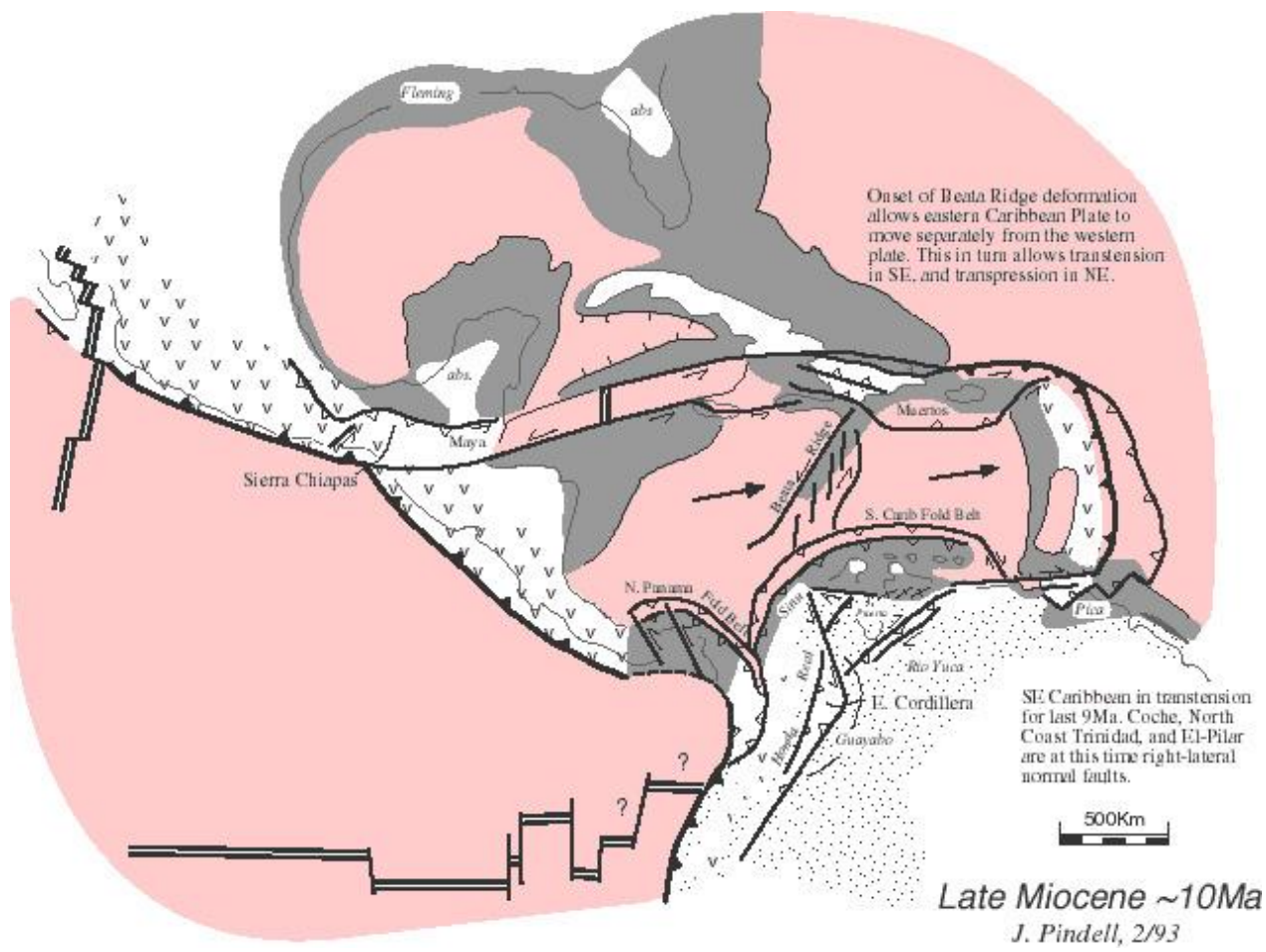
b) Middle Eocene stage (49 Ma) of the plate reconstruction done for the circum-North Andean region (Pindell, 1993).



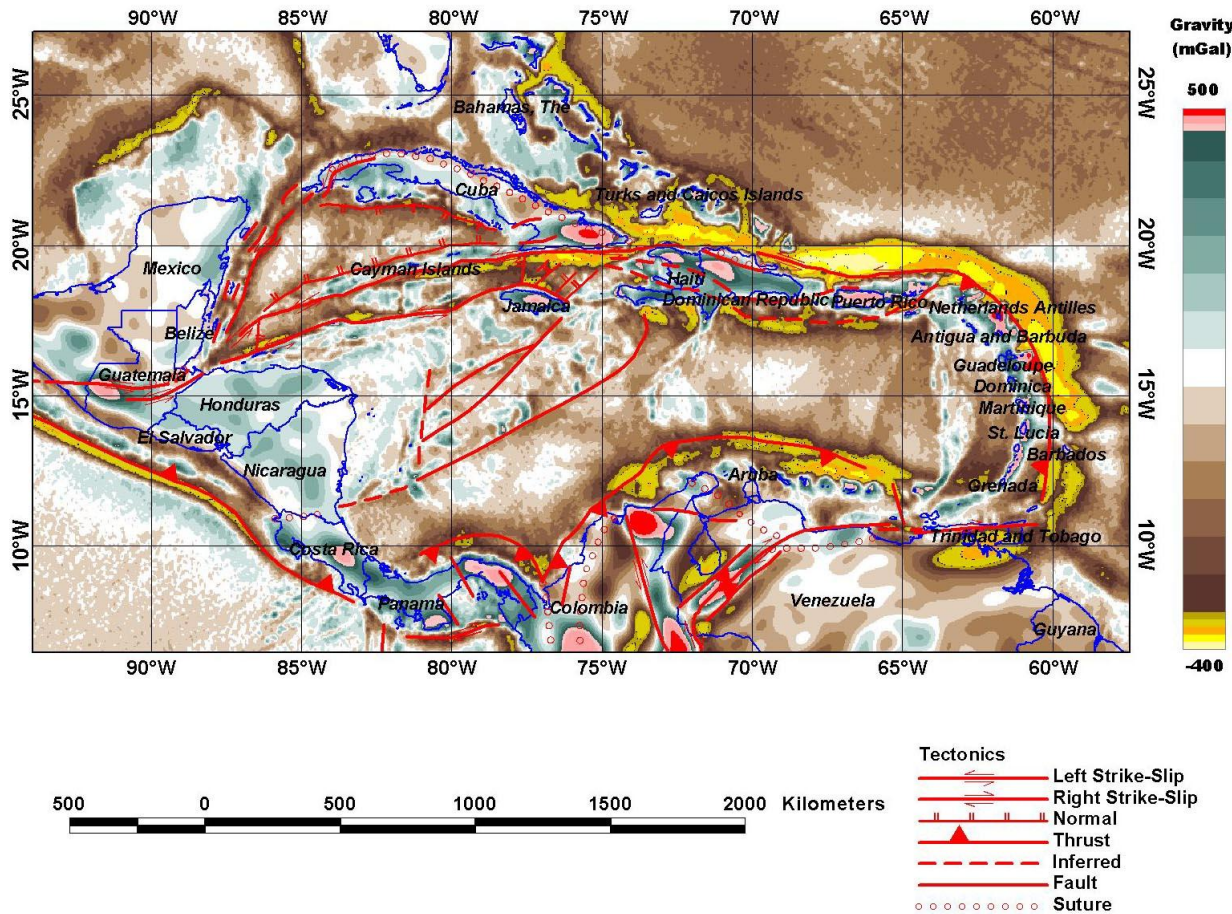
c) Early Oligocene stage (35 Ma) of the plate reconstruction done for the circum-North Andean region (Pindell, 1993).



d) Early Miocene stage (21 Ma) of the plate reconstruction done for the circum-North Andean region (Pindell, 1993).



e) Late Miocene stage (10 Ma) of the plate reconstruction done for the circum-North Andean region (Pindell, 1993).



f) Present-day stage (0 Ma) of the plate configuration in the circum-North Andean region (Allen, 2002).

Figures 1c-e further allow to see that the overall dextral transpressional regime in the Northern Andes, which is driven by relative movements of the Caribbean and South American systems, gains a complexity as the Panama - South America convergence of progressively evolves into more advanced stage during the Early Oligocene - Late Miocene time period.

The overall dextral transpression in the North Andean region is further documented by **Fig.2**, which shows the present-day σ_1 stress trajectories interpreted from earthquake focal mechanisms by Arcila *et al.* (2000). The σ_1 stress deflection between the western and eastern sides of the map indicates relatively low-friction interface between the two converging plate systems, i.e. the Caribbean, Cocos and Nazca system advancing from the west and the South American Plate advancing from the east. In particular, the $54 \text{ mm} \text{y}^{-1}$ eastward advance of the Nazca Plate towards the South American Plate creates an important dextral transpression along the NE-SW interface of these two plates (see the inset in **Fig. 2** for geometric relationships).

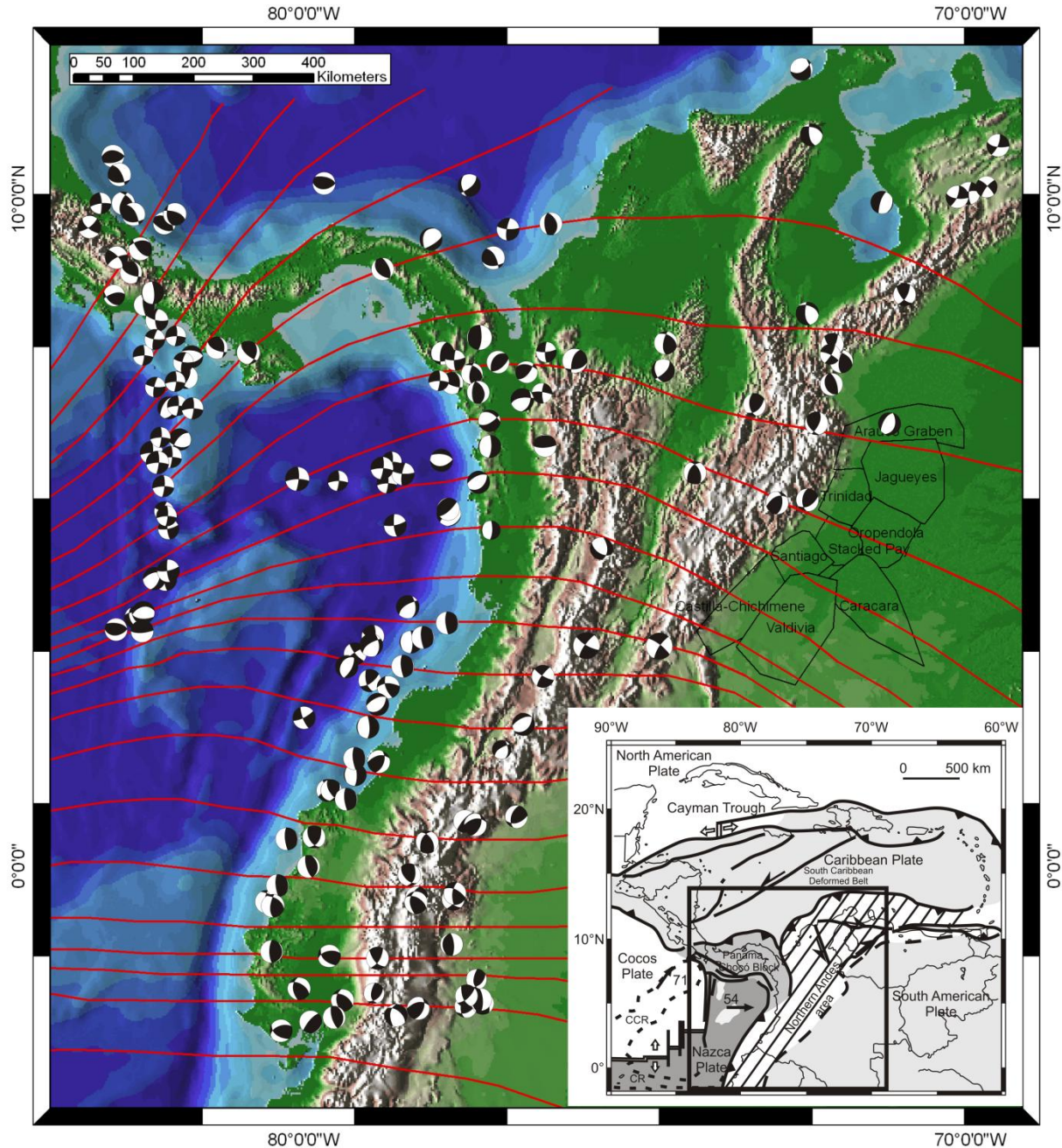


Fig. 2. Extrapolated in situ σ_1 stress trajectories (red) based on earthquake focal mechanism data in circum-North Andean region (Arcila *et al.*, 2000). Note that the Eastern Cordillera is affected by dextral transpression, the strike-slip component of which decreases from the south to the north. Inset shows major tectonic elements of the Caribbean Region and Northern Andes (Cortés & Angelier, 2005a). Rectangle indicates the location of main figure.

Such stress control of the transpressional interface has been recognized in numerous segments of orogenic belts such as the Taiwan Thrustbelt (Huchon *et al.*, 1986), the West Carpathians (Nemčok, 1993; **Fig. 3**) and the South Wales Variscan (Gayer *et al.*, 1998; **Fig. 4**).

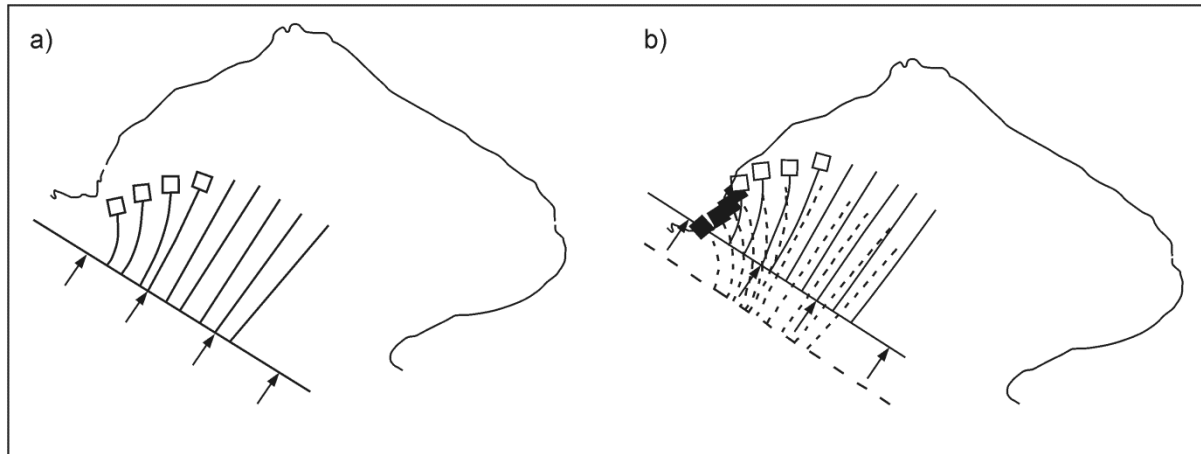


Fig. 3. Orogen advance with indication of rotated σ_1 stress record in older strata in the West Carpathians (Nemčok, 1993). Arrows – motion of orogenic hinterland advancing from stage (a) to stage (b); bold lines – younger σ_1 trajectories; dashed lines – older σ_1 trajectories. Outlined squares in stage (a) show σ_1 stress pattern of period (a). Those stress records are progressively rotated in younger stage (b) (black squares) and the new σ_1 stress pattern of period (b) (outlined squares) is shown.

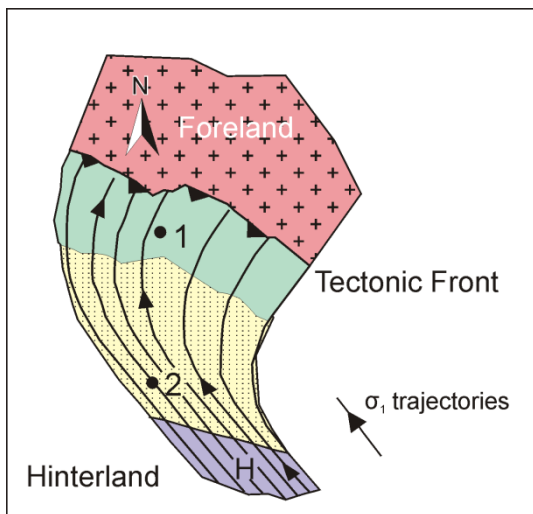


Fig. 4. Simplified model of curvilinear σ_1 stress trajectories in Variscan transpressional wedge, South Wales, from foreland, through coal-bearing foreland basin (green), and thicker part of wedge (yellow), to hinterland (Gayer *et al.*, 1998).

The problem with recognition of transpression-indicative stress pattern can appear when we have a relatively limited amount of locations with data allowing the paleostress calculation. Robust studies such as that of the West Carpathians by Nemčok (1993) (**Fig. 5**), however, can serve as an analog.

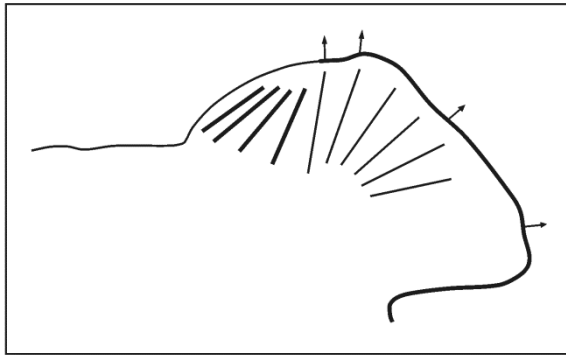


Fig. 5. Sketch of the West Carpathian σ_1 stress trajectories in orogen regions affected by tectonic escape and regions with still active thrusting along the orogenic front (Nemčok, 1993). The front of the orogen is indicated by a thin line in areas of inactive thrusting and by a bold line in areas of active thrusting. Sketched σ_1 stress trajectories are indicated by bold lines in regions of tectonic escape and by thin lines in regions behind active thrusting.

The robust studies would help to explain an apparent mismatch between the E-W trending σ_1 stresses in the southern portion of the Eastern Cordillera-Llanos foreland basin system and NW-SE trending σ_1 stresses in the northern portion, which are recognized from in-situ stress data coming from industrial wells, as a mirror image of the stress situation shown in **Fig. 5**. The comparison between fully and partially defined stress fields of the West Carpathians and Eastern Cordillera, respectively, allows one to imply that the overall dextral transpression in the Eastern Cordillera-Llanos foreland basin system has a strike-slip (simple shear) component, which decreases from the south to the north along the Eastern Cordilleran strike, and orthogonal contraction (pure shear) component, which increases from the south to the north along the Eastern Cordilleran strike.

Although the amount of fault-striae data from the Guaduas Syncline-Apulo region and Sabana de Bogotá Plateau used for paleostress calculations by Cortés & Angelier (2005b) does not represent as rigorous data coverage as that of Nemčok (1993) and Nemčok *et al.* (1998, 2007), a comparison of their results with the stress model interpretation shown in **Fig. 5**, allows one to interpret the existence of the dextral transpressional regime with spatially and temporally changing ratio of simple and pure shear components as most likely characterizing the entire Paleocene-present-day time span.

The following paleostress tensors calculated by Cortés & Angelier (2005b), who recognized:

- 1) the Cretaceous – Eocene tensor characterized by the E-W to WSW-ENE trending σ_1 stress;
- 2) a bit younger tensor with σ_1 stress having the NW-SE trend; and
- 3) the Oligocene-Pliocene tensor characterized by the WNW-ESE trending σ_1 stress,

all fit with the interpretation of the overall dextral transpressional regime.

Before discussing stratigraphic data from the Llanos foreland basin, it would be useful to look at [analog material modeling](#) focused at main thrustbelt-controlling factors (Macedo & Marshak, 1999) and apply the modeling results to the Eastern Cordillera.

The modeling shows that one can distinguish the foreland basin-control from the indenter-control on the development of the orogenic salient, such as the one formed in the northern part of the Eastern Cordillera of Colombia. While the modeled orogen trend lines converge at end points of the basin-controlled salient, they diverge at the end points of the indenter-controlled salient ([Fig. 6](#)).

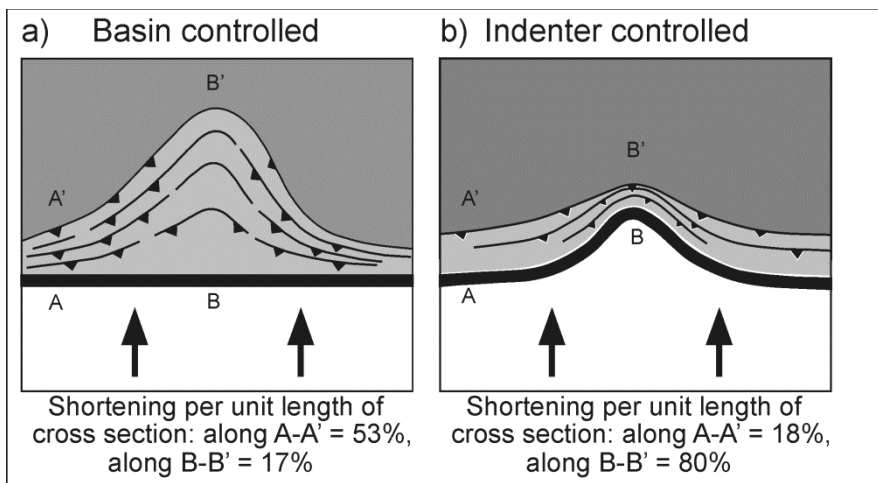


Fig. 6. Fundamental contrasts between basin-controlled salients and indenter-controlled salients (Macedo & Marshak, 1999). a) The basin-controlled salient is characterized by trend lines converging at end points, emphasizing that the thicker the foreland basin fill, the wider the thrust sheets accreted to the frontal thrustbelt (see [Fig. 7](#)). b) The indenter-controlled salient is characterized by trend lines diverging at end points, emphasizing that trend lines converge in front of the indentation point.

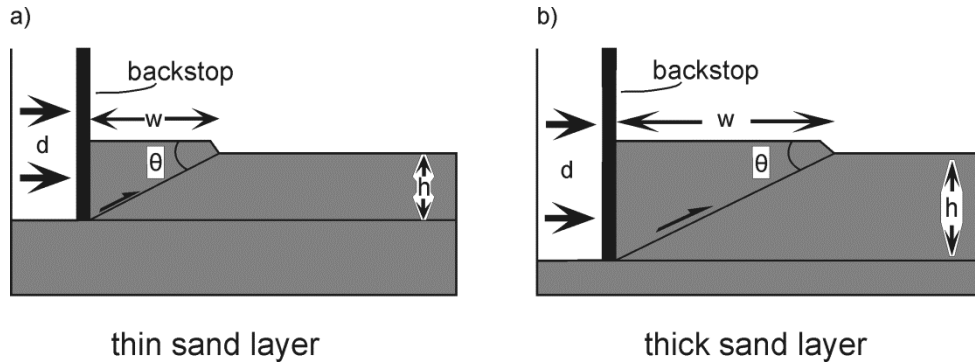


Fig. 7. Cross-section comparison of the effect of layer thickness on the width of a thrust sheet (Macedo & Marshak, 1999). Assuming the same ramp angle, controlled by the angle of internal friction of deforming material, the width of thrust sheet increases with layer thickness (see also Marshak & Wilkerson, 1992).

In order to choose between basin and indenter control, one has to draw a system of trend lines for the Eastern Cordillera, using the geological map from **Fig. 8**, which provides the fault traces and anticlinal and synclinal axes as guidelines. The resultant trend line map is shown in **Fig. 9**. A comparison to **Fig. 6** and other orogenic analogs shown in **Fig. 10** indicates that the trend line pattern can be characterized as a pattern converging to both end points, which indicates basin control of the orogenic salient development.

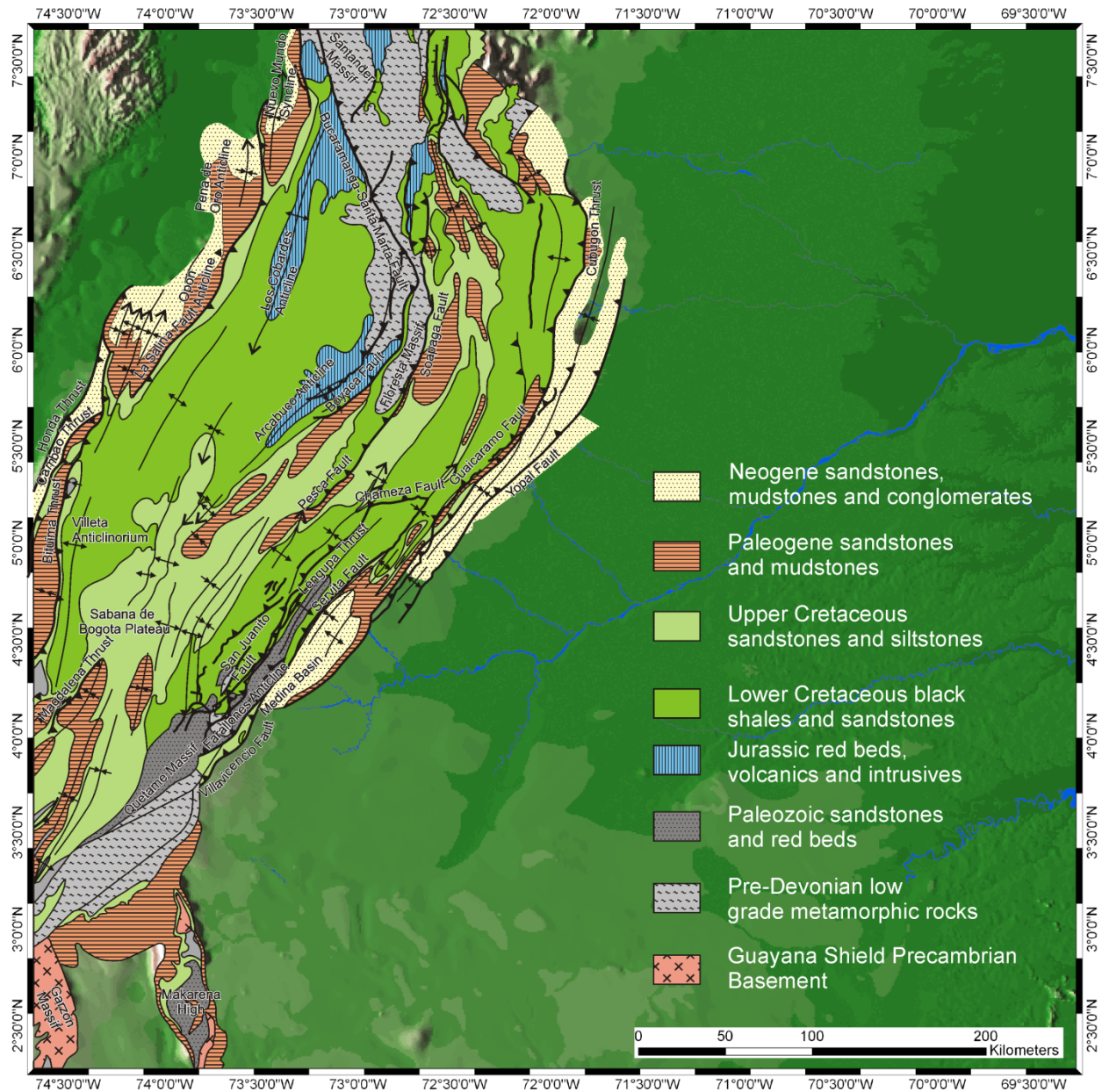


Fig. 8. Geologic map of the Eastern Cordillera with an indication of main faults and tectonic features (modified from Mora *et al.*, 2006, 2008, 2010; Parra *et al.*, 2009).

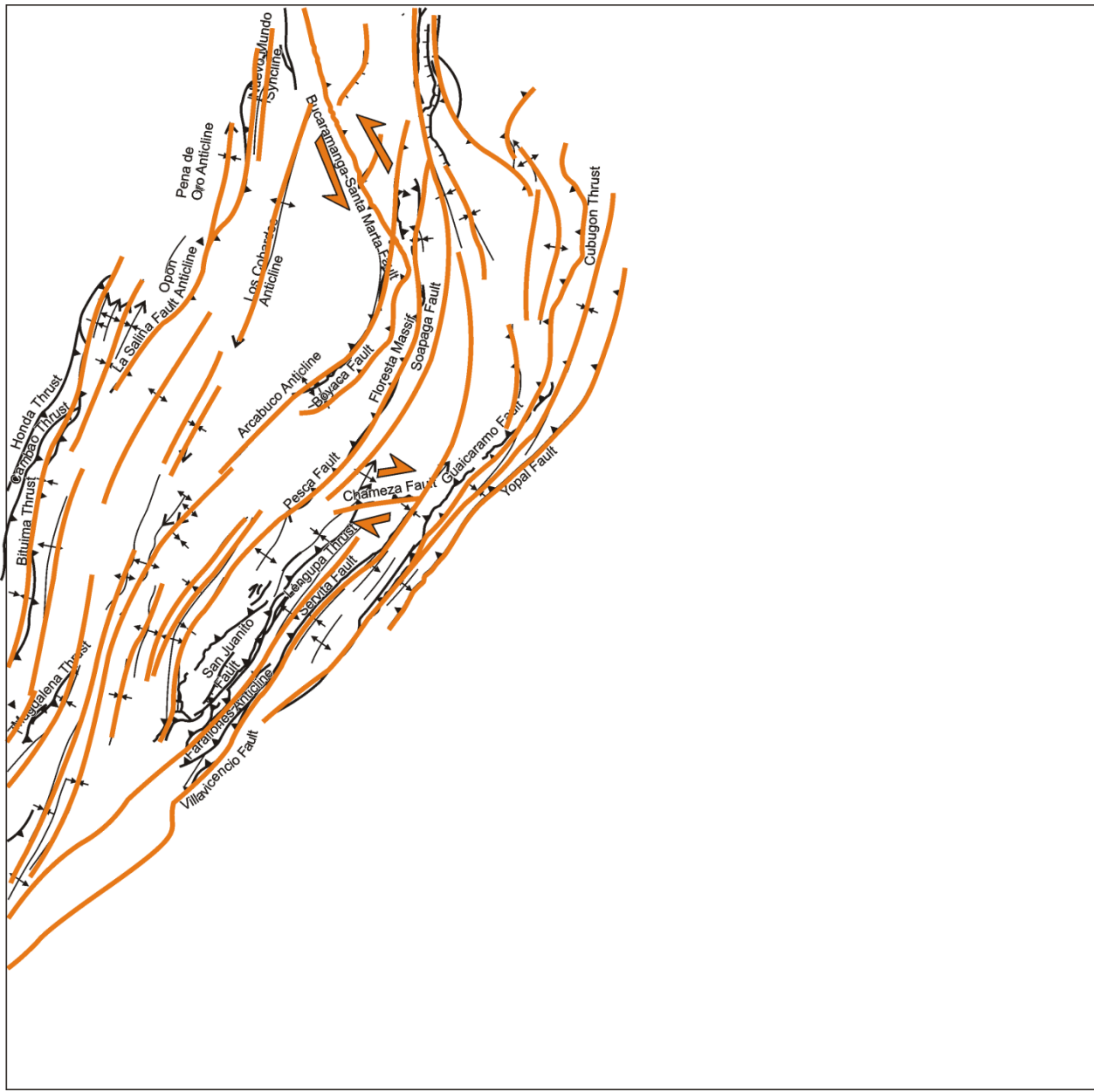


Fig. 9. Trend line map drafted using the fault traces and fold axes from Fig. 8.

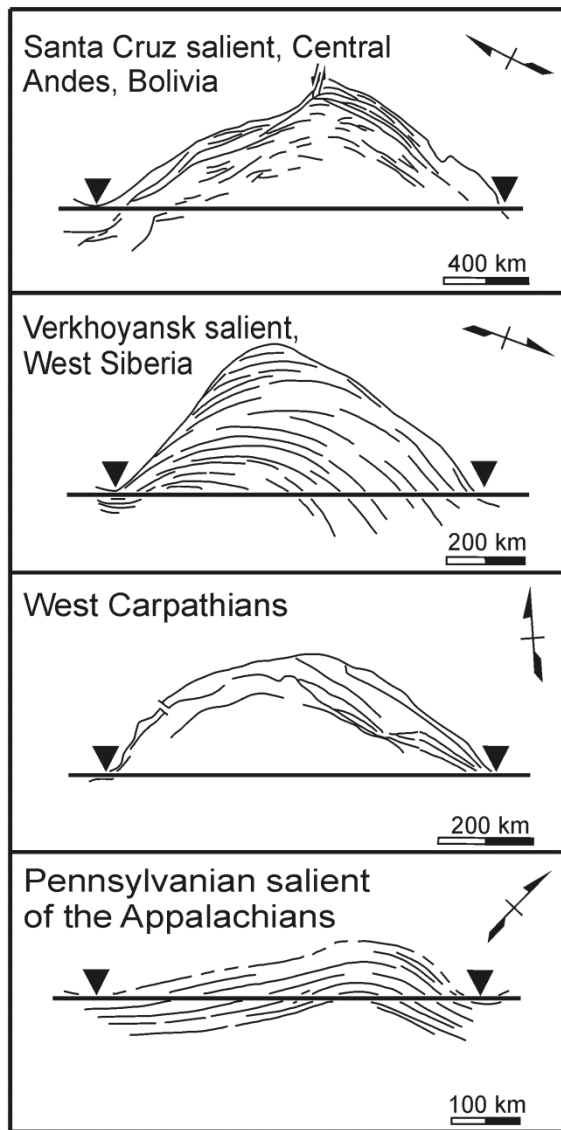


Fig. 10. Map views of trend line patterns of selected orogenic belts analogous to the Eastern Cordillera (modified from Macedo & Marshak, 1999). The Santa Cruz case indicates basin control and partially margin geometry control. The Verkhoyansk case indicates a basin control and some buttressing effect at one end point. The West Carpathians case indicates basin control with some margin geometry control. The Pennsylvanian case indicates basin control with some margin geometry control.

Proving a dominant basin-controlling role in shaping the geometry of the Eastern Cordillera allows us to use a well known behavior of the Western Carpathians as an analog for the **depositional history of the foreland basin** related to obliquely closing the orogen-foreland basin system.

The ALCAPA terrane of the Western Carpathians (**Fig. 11**) during its Eggenburgian – middle Badenian (19-15.5 Ma) development history (**Fig. 12**) could then serve as a rough mirror image analog for the Eastern Cordillera during its Paleocene – present-day development history.

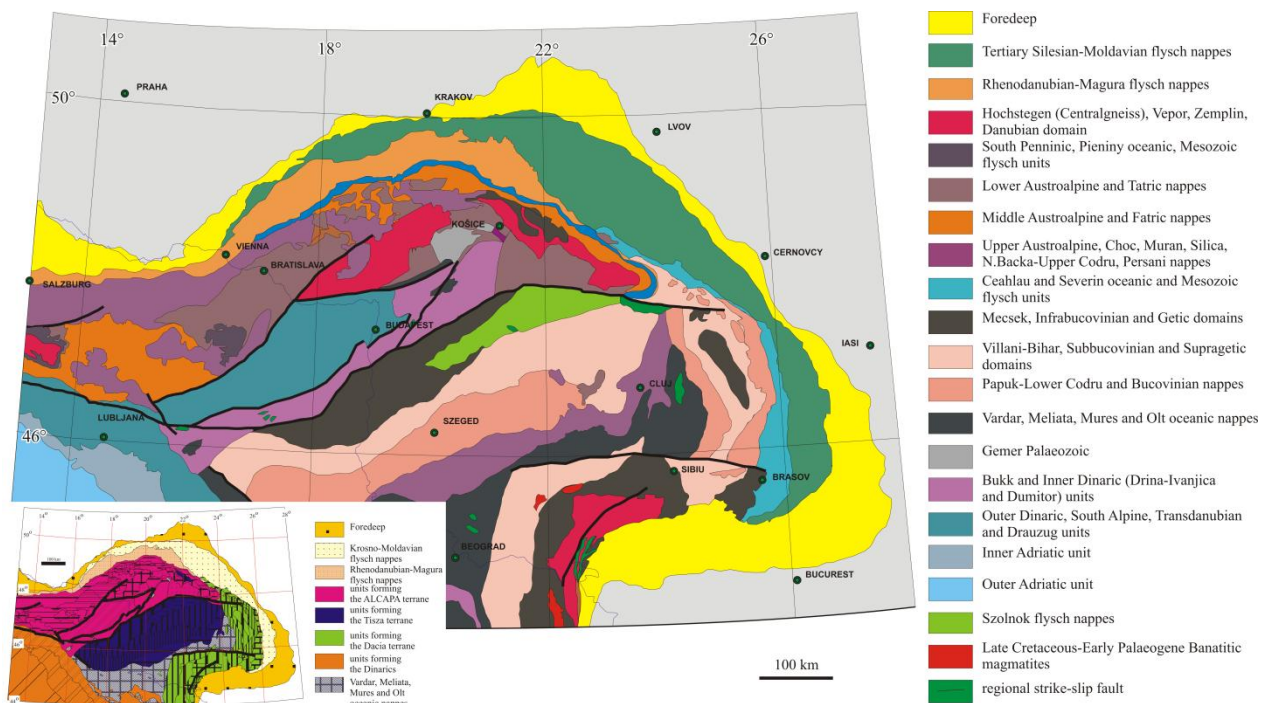


Fig. 11. Block pattern map of the Carpathian – Pannonian region based on correlation of Paleozoic – Mesozoic facies (modified after Csontos *et al.*, 1992). The ALCAPA terrane in inset is indicated by purple.

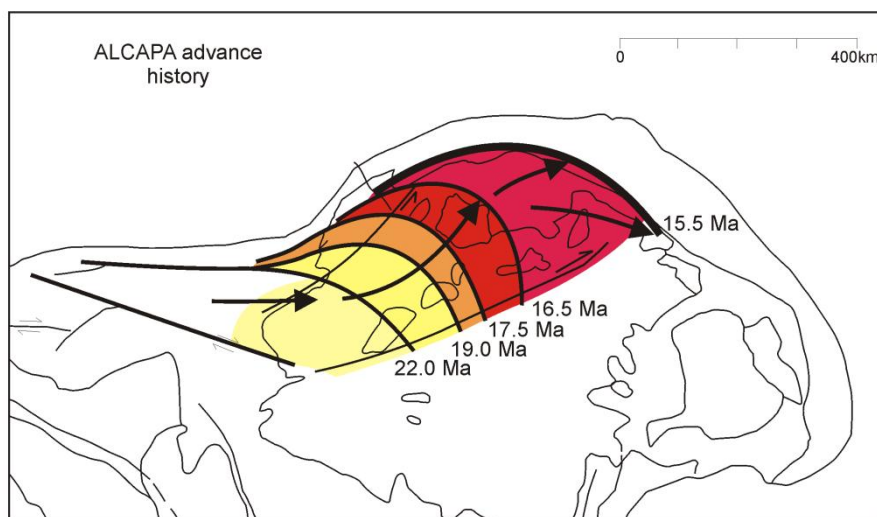


Fig. 12. ALCAPA terrane advance reconstruction since Late Oligocene, based on presumed proportional relation between amounts of lateral foredeep depocenter migration and outward motions of the ALCAPA terrane (Meulenkamp *et al.*, 1996).

The ALCAPA advance history, which was reconstructed by Meulenkamp *et al.* (1996) using stratigraphic constraints, roughly matches with that of Ellouz & Roca (1994), done by reconstructing serial balanced cross sections, that of Nemčok *et al.* (2006), done by using the activity time periods of numerous intra-Carpathian faults as constraints, and that of Nemčok *et al.* 1999 using detailed calculations from five balanced cross sections through the northern portion of the West Carpathians (**Fig. 13**). The oblique closure of the West Carpathians-foreland basin system has been proven by numerous studies listing the age of the youngest sediments overridden by the Carpathian frontal thrust and the oldest sediments sealing its propagation tip (e.g., Jiříček, 1979; Krus & Šutora, 1986; Meulenkamp *et al.*, 1996; Nemčok *et al.*, 1998b, 2006; **Fig. 14**).

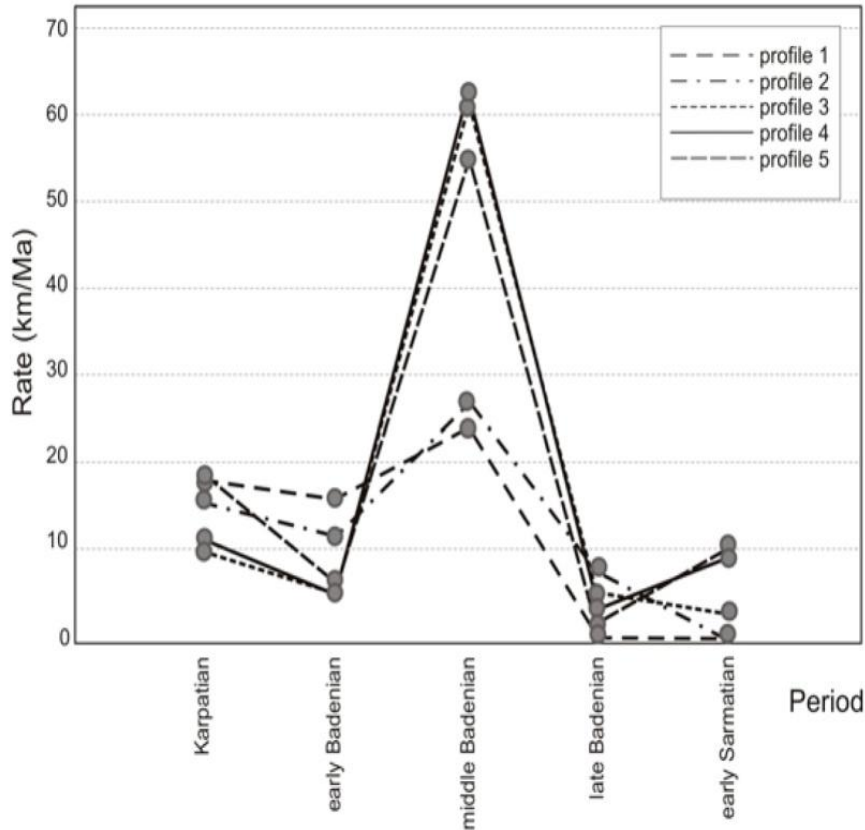


Fig. 13. Neogene West Carpathian accretionary wedge advance rates derived from balanced cross sections (data from Nemčok *et al.*, 1999). Serial profiles 1 to 5 cut the West Carpathian thrustbelt in direction from W to E. Note that western profiles undergo the thrusting termination first. The termination time of thrusting becomes younger as one goes from west to east.

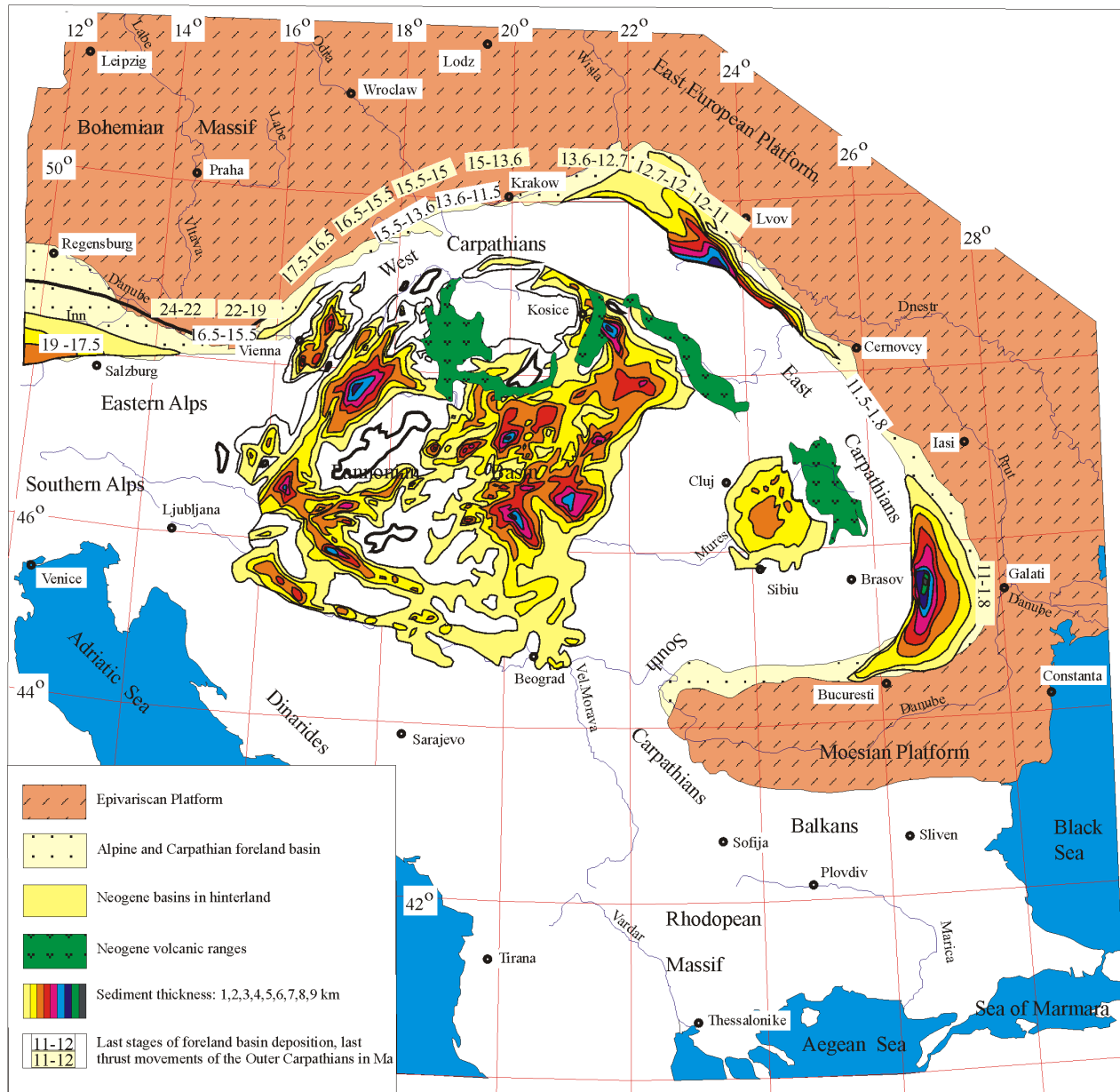


Fig. 14. Tertiary sediment thickness map of the Carpathian–Pannonian region with indications of the last period of foreland molassic deposition and thrusting of the Outer Carpathians (modified by Nemčok *et al.*, 1998 after Ksiazkiewicz, 1960; Buday, 1965; Jurková, 1971; Vjalov, 1974; Jiříček, 1979; Stráník *et al.*, 1979; Steininger *et al.*, 1984; Benada, 1986; Krus & Šutora, 1986; Meulenkamp *et al.*, 1996). The total Neogene sediment thickness distribution is based on the relatively dense network of industrial bore holes, reflection seismic and gravity data. Note two series of numeric values. Those on yellow background show the age of the last activity of the frontal Carpathian thrust. Those on white background show the age of the last important subsidence in the foreland basin.

Fig. 14 indicates that the sinistral transpressional (oblique) closure of the West Carpathians-foreland basin system results in the timing of the last important subsidence in the foreland basin younging from west to east, in some kind of linear relationship with the younging of the last activity of the frontal Carpathian thrust. The thickest total Neogene thickness of the foreland

basin fill is located in front of the advance vector of the ALCAPA terrane (compare **Figs. 14** and **12**).

We believe that the eastward traveling last important subsidence centers are controlled by the stress distribution in the orogen-foreland system, which is shown in **Fig. 15**. **Fig. 15** shows how the flexure-controlled subsidence during the oblique closure of the convergent system should vary due to the areal distribution of the vertical loading plus horizontal push direction, which both control the extent of the foreland plate flexure.

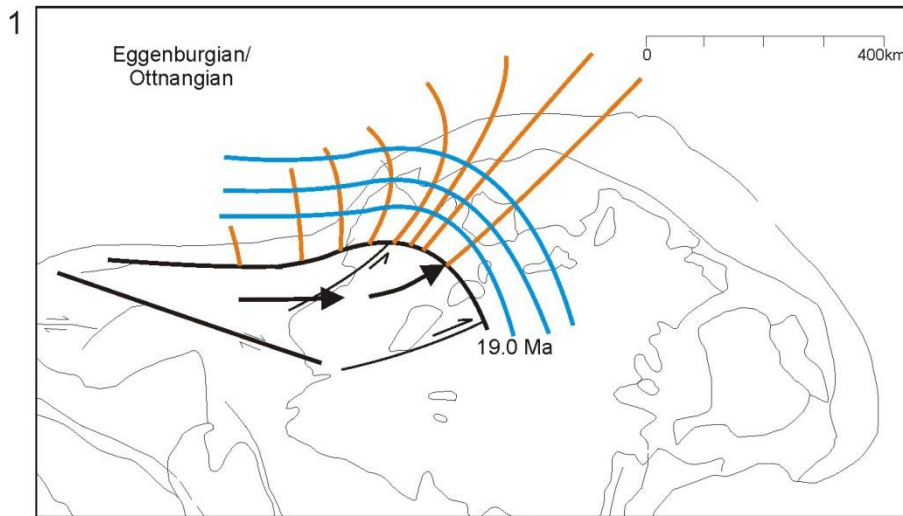
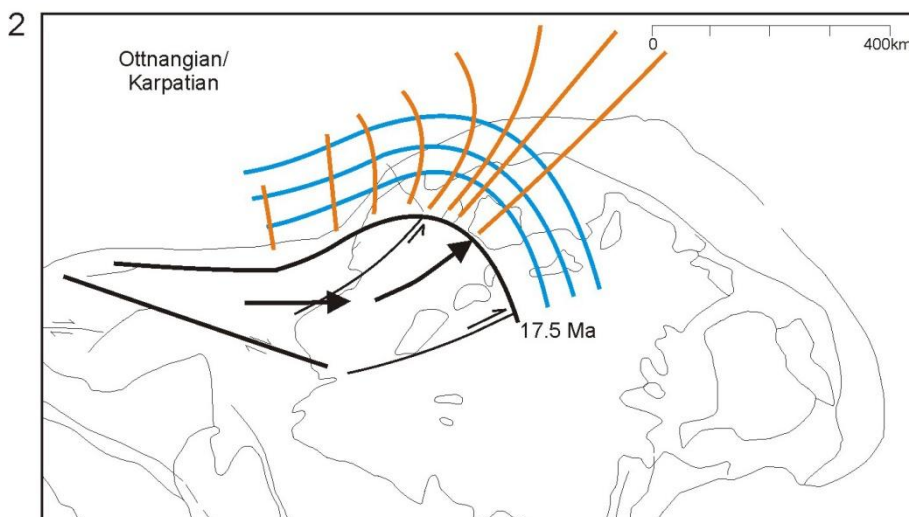
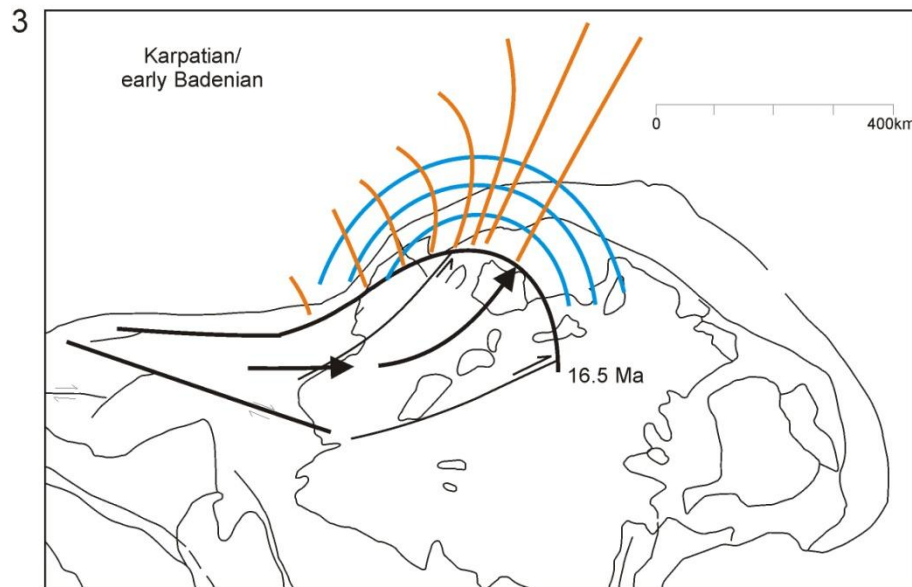


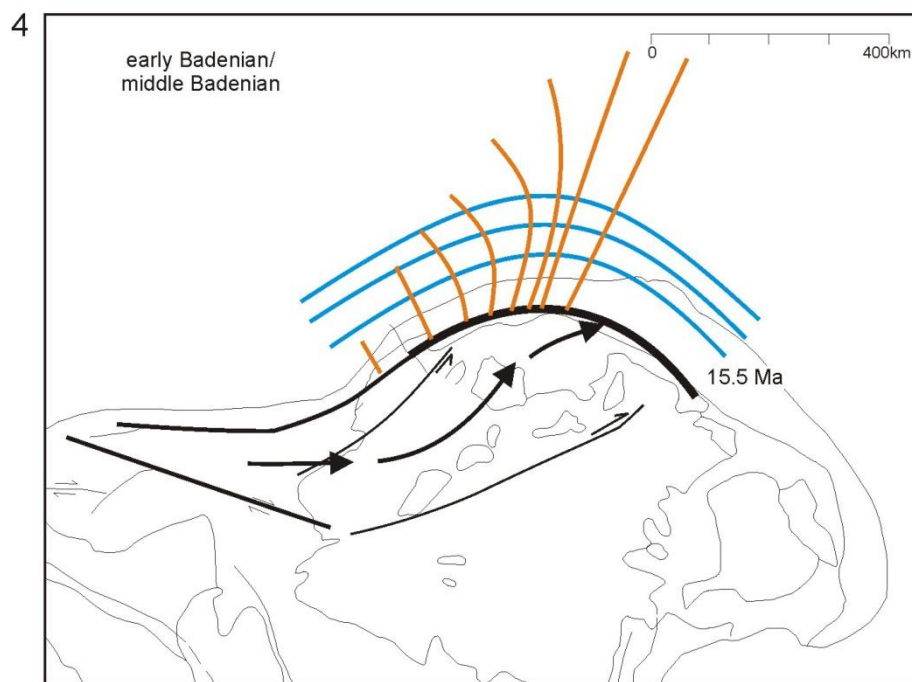
Fig. 15. a) Eggenburgian/Ottnangian boundary snap shot of the ALCAPA advance with sketch of vertical loading distribution (blue lines) and horizontal push distribution (orange lines).



b) Ottnangian/Karpatian boundary snap shot of the ALCAPA advance with sketch of vertical loading distribution (blue lines) and horizontal push distribution (orange lines).



c) Karpatian/early Badenian boundary snap shot of the ALCAPA advance with sketch of vertical loading distribution (blue lines) and horizontal push distribution (orange lines).



d) early/middle Badenian boundary snap shot of the ALCAPA advance with sketch of vertical loading distribution (blue lines) and horizontal push distribution (orange lines).

A mirror image to the eastward younging important subsidence of the West Carpathian foreland basin due to the overall sinistral transpressional closure of the West Carpathian-foreland basin system should come from the dextrally closing Eastern Cordillera-Llanos foreland basin system. Indeed, the maps showing the depocenter location for the time periods of deposition of the Carbonera and León formations, and sub-units 4, 3 and 2 of the Guayabo Formation represent such mirror image (**Fig. 16**). This indicates a dextral transpressional closure of the system, in accordance with plate reconstruction data, paleostress data and in situ stress data.

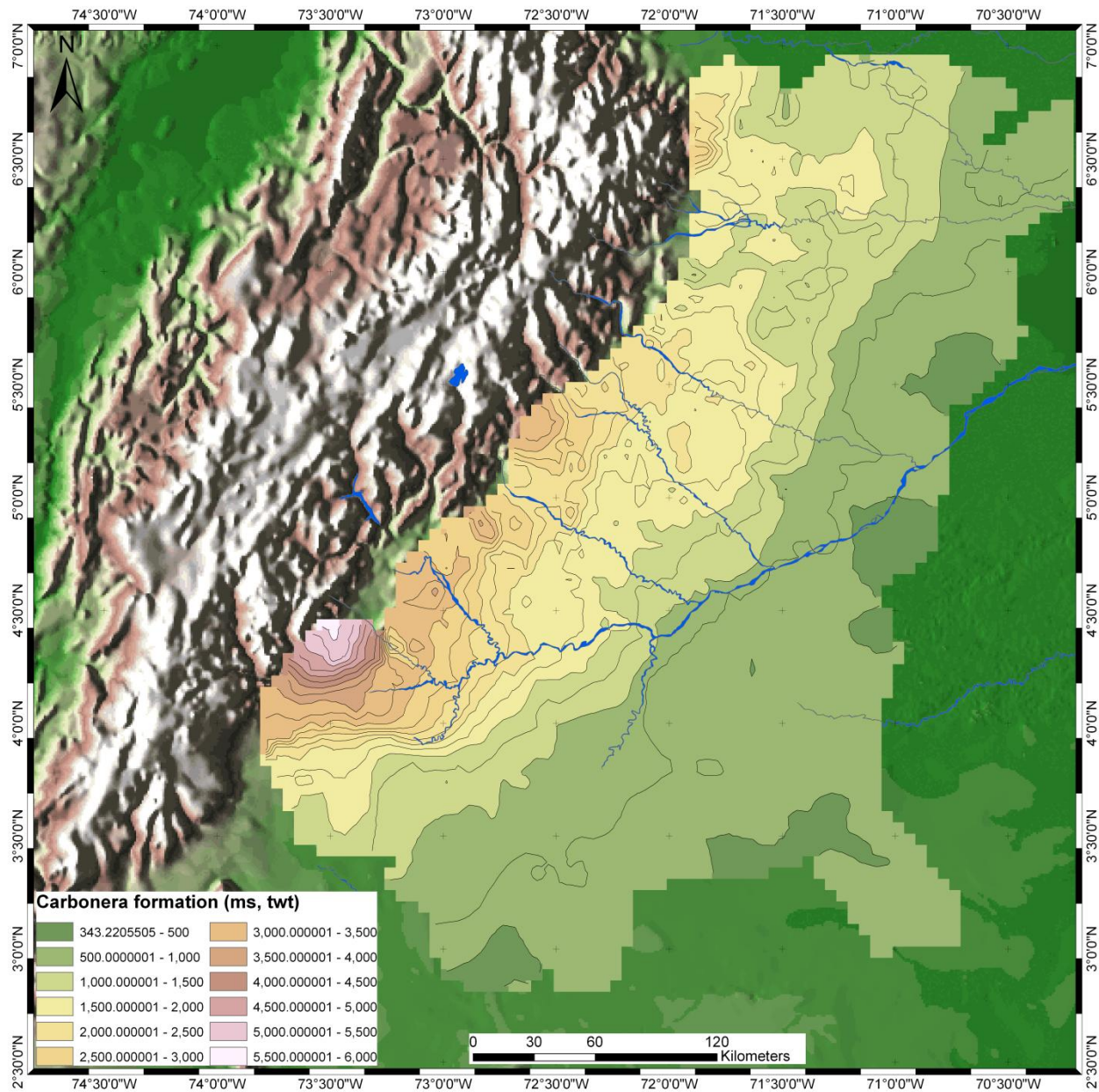
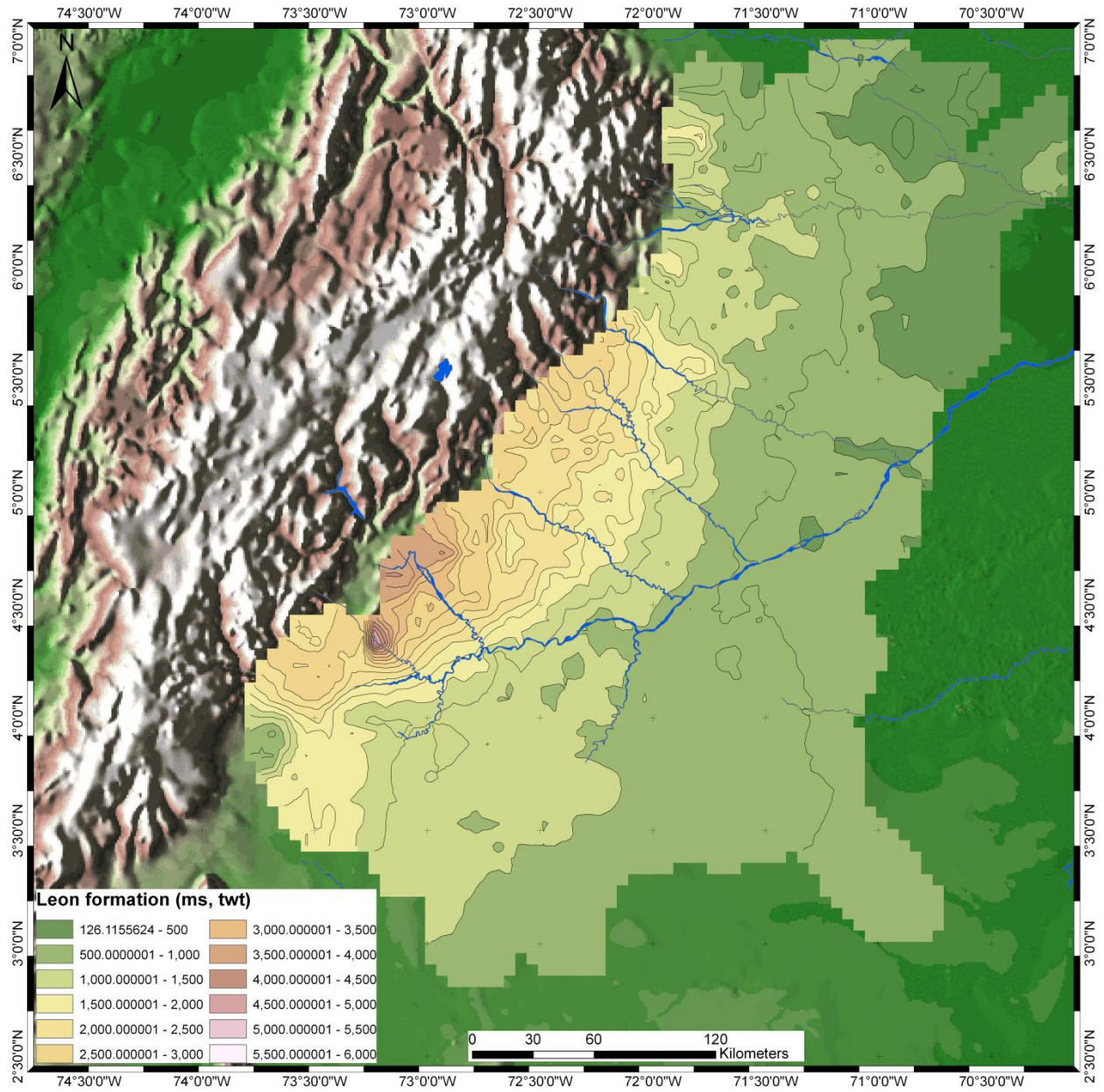
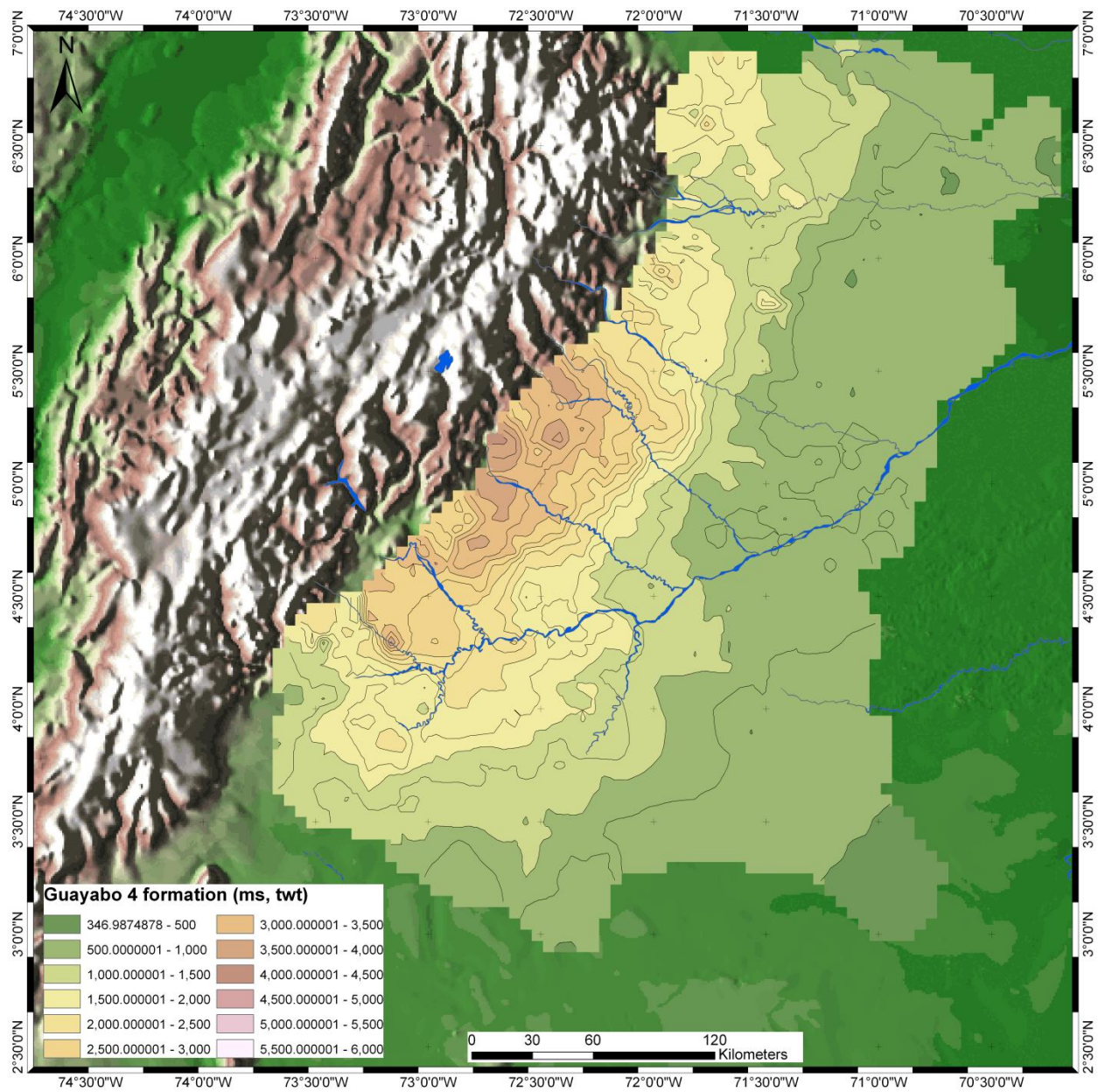


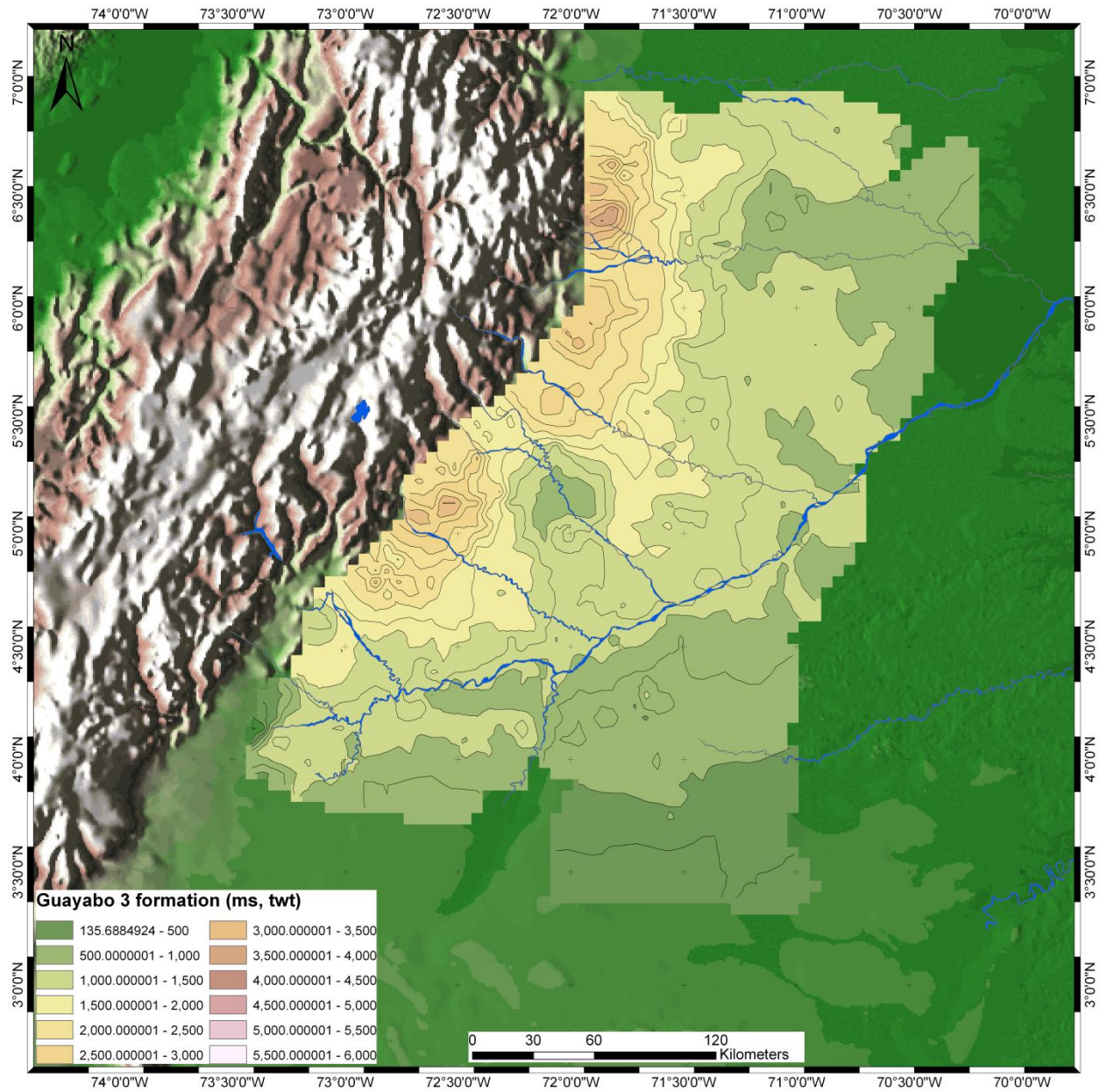
Fig. 16. a) Thickness distribution of the Carbonera Formation.



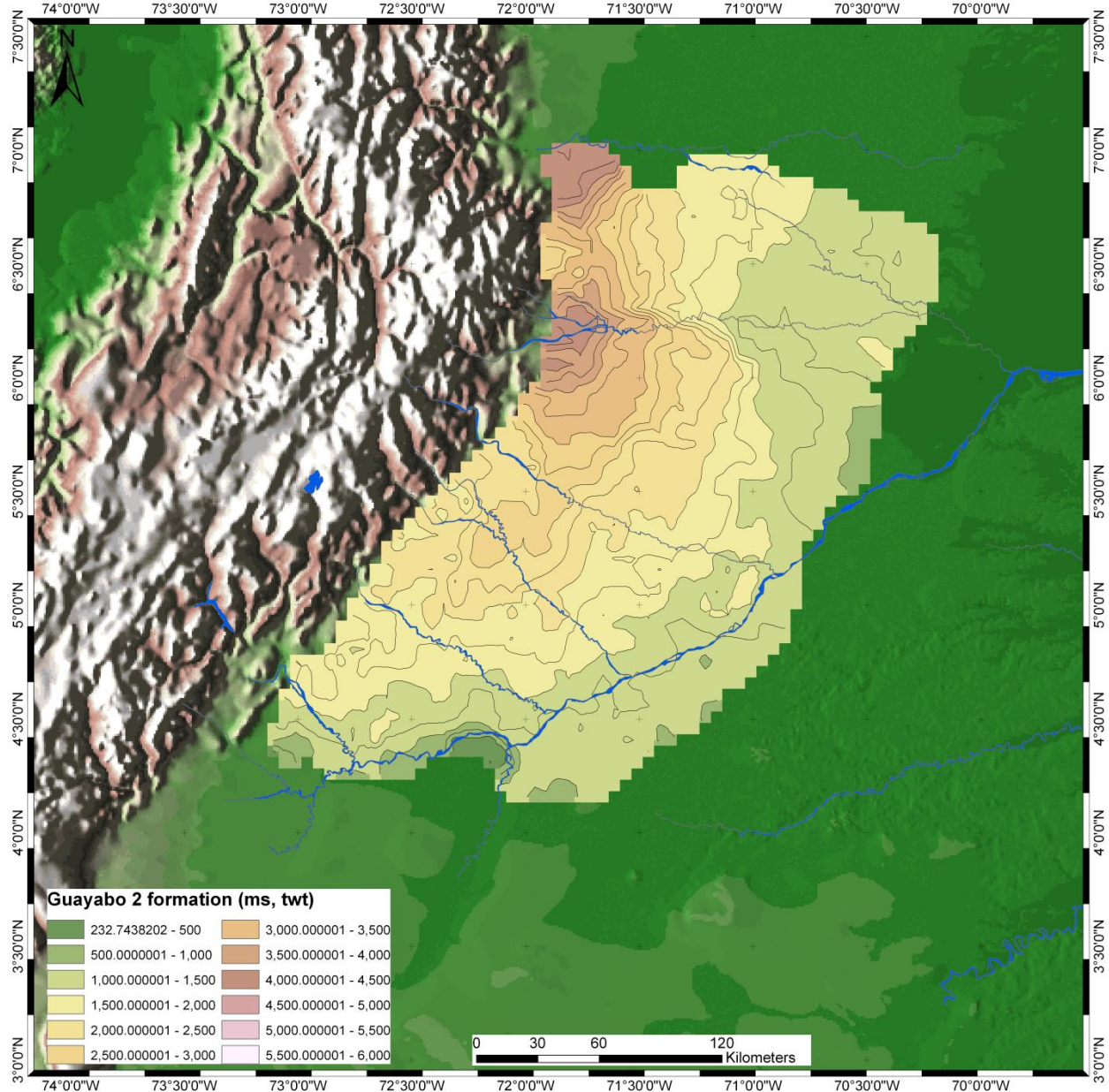
b) Thickness distribution of the León Formation.



c) Thickness distribution of the sub-unit 4 of the Guayabo Formation.



d) Thickness distribution of the sub-unit 3 of the Guayabo Formation.



e) Thickness distribution of the sub-unit 2 of the Guayabo Formation.

The chain of implications discussed in this text can be finished with two remaining steps. The first step involves the interpretation of the orogenic loading for the Eastern Cordillera-Llanos foreland system, following the West Carpathian analog (**Fig. 17**).

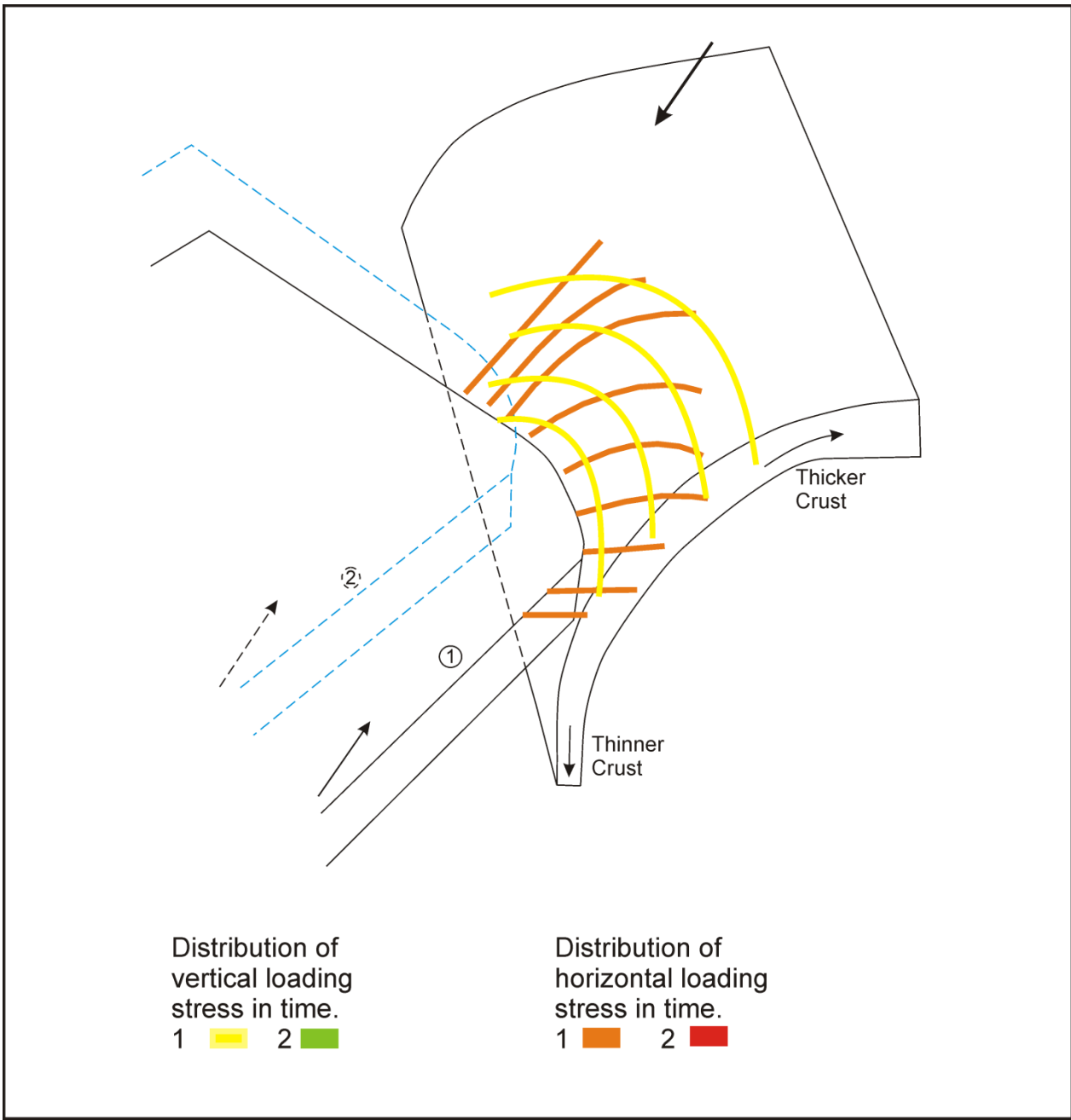
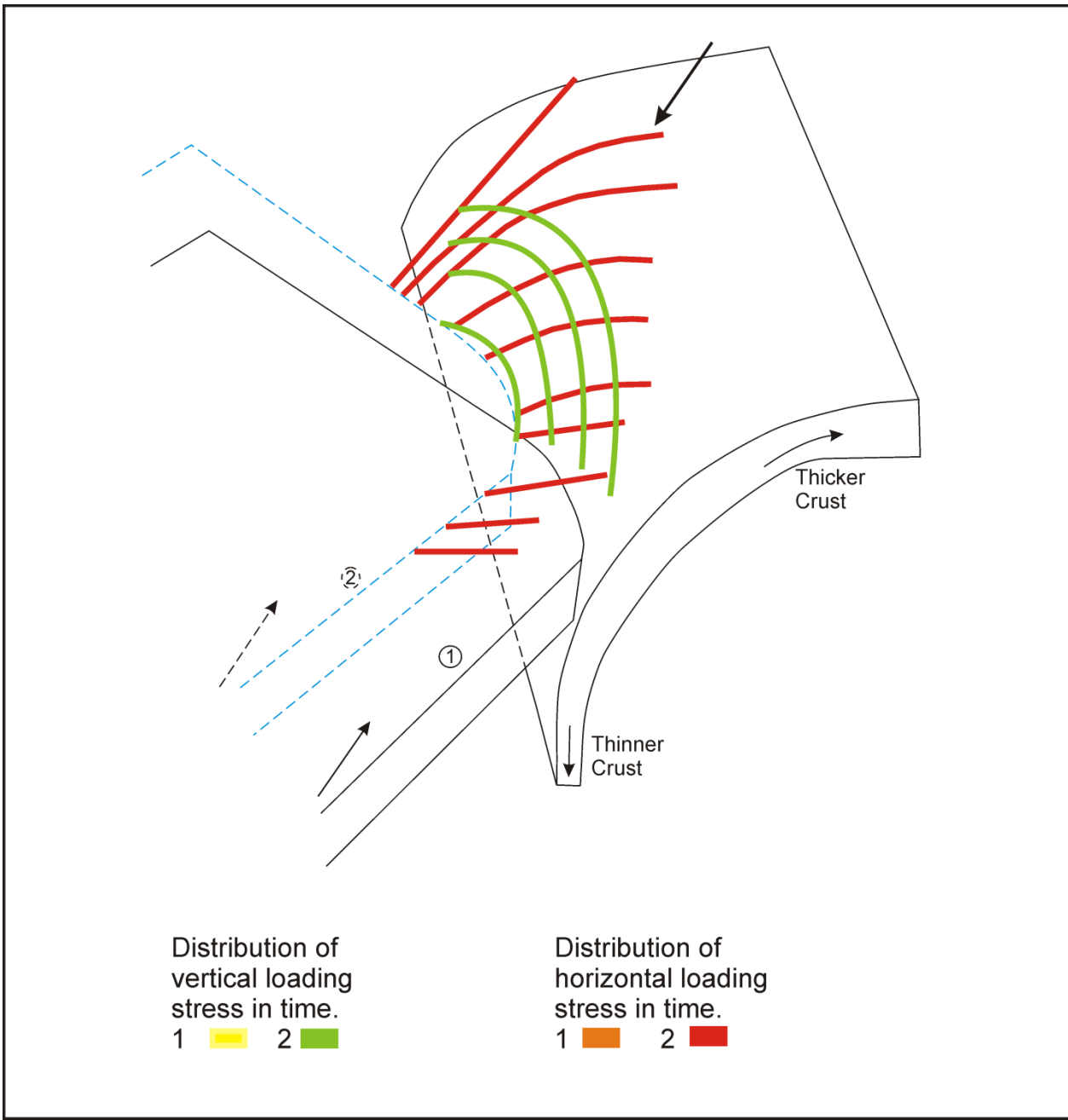


Fig. 17. a) Stage 1 of the schematized oblique closure of the Eastern Cordillera-Llanos foreland basin system. Note the distribution of the vertical loading of the flexing foreland plate (yellow lines) and horizontal push exerted by the advance trend of the advancing orogen (orange lines). Note that the geometry of the overridden plate resembles a subduction zone, which is not a correct representation for the retro-wedge but it helps to exaggerate the difference between the flexing overridden crust and the overriding orogenic crust for easier understanding of flexural controls.



b) Stage 2 of the schematized oblique closure of the Eastern Cordillera-Llanos foreland basin system. Note the distribution of the vertical loading of the flexing foreland plate (green lines) and horizontal push exerted by the advance trend of the advancing orogen (red lines). Note that geometry of the overridden plate resembles a subduction zone, which is not a correct representation of the retro-wedge but it helps to exaggerate the difference between flexing overridden crust and the overriding orogenic crust for easier understanding of flexural controls.

The second step involves an assumption that the crust is thinned by a system of grabens and half-grabens of both Paleozoic and Cretaceous rift systems, controlling the foreland crust thinning in direction from east to west. Because the closure of the Eastern Cordillera-Llanos foreland basin system is oblique the thickness of the foreland crust overridden by the orogenic front becomes

progressively thinner from south to north along the Eastern Cordillera-Llanos foreland basin interface.